Journal of Nuclear Materials 385 (2009) 178–183

Contents lists available at ScienceDirect

Journal of Nuclear Materials

journal homepage: www.elsevier.com/locate/jnucmat

# Behavior of Si impurity in Np–Am–MOX fuel irradiated in the experimental fast reactor Joyo

Koji Maeda [a,*], Shinji Sasaki [a], Masato Kato [b], Yoshiyuki Kihara [b]

[a] Oarai Research and Development Center, Japan Atomic Energy Agency, 4002 Narita, Oarai, Ibaraki 311-1393, Japan
[b] Nuclear Fuel Cycle Engineering Research Institute, Japan Atomic Energy Agency, 4-33 Muramatsu, Tokai-mura, Naka-gun, Ibaraki 319-1194, Japan

ARTICLE INFO

*PACS:*
28.41.Bm

ABSTRACT

The irradiation behavior of uranium–plutonium mixed oxide fuels containing a large amount of silicon impurity was examined by post-irradiation examination. Influences of Si impurity on fuel restructuring and cladding attack were investigated in detail. Si impurity, along with Am, Pu and O were transported by spherical pores and cylindrical tubular pores to the fuel center during fuel restructuring of the Np–Am–MOX fuel, where a eutectic reaction of fuel and Si-rich inclusions occurred. After fuel restructuring of the Np–Am–MOX fuel, Si-rich inclusions without fuel constituents were agglomerated at fuel crack openings where shallow attacks on the inner wall of the cladding were seen. Such shallow attacks on the inner wall of the cladding were likewise observed near the location of fuel cracks in long-term steady-state irradiated MOX fuels. Evidence of these shallow attacks on the inner wall of the cladding remained after fuel restructuring in normal MOX fuel. However, grain boundary corrosion of the cladding inner wall at the opening of the fuel cracks was selective and was marked in MOX fuel at higher oxygen potential by the release of reactive fission products such as Cs and Te in comparison with other regions of cladding wall.



## 1. Introduction

A uranium and plutonium mixed oxide (MOX) fuel containing minor actinides was used in two short-term irradiation tests of the Am-1 experiment [1] which were finished in 2006. The objective of the tests was to research thermal behavior of MOX fuels containing minor actinides such as fuel restructuring and minor actinide redistribution. Three fuel pins containing 2% neptunium and 2% americium MOX fuel pellets (Np–Am–MOX) were supplied for testing after which they were subjected to post-irradiation examinations (PIE).

In ceramography of the fuel pin used in the first test, evidence of a $SiO_2$–MOX reaction around the central void was detected, and influence of Si impurity on fuel restructuring in the Np–Am–MOX fuel was suggested [2]. In the second test, Si-rich compounds were agglomerated at the fuel crack opening, where a shallow attack on the cladding inner wall was observed. This was unexpected irradiation behavior for Si impurity in the Np–Am–MOX fuel.

It is particularly-important to evaluate the behavior of Si impurity which occurred in an early stage of irradiation, because it will be closely linked to the thermal design of fuel pins. A detailed investigation of Si impurity behavior was made on the Np–Am–MOX fuel pin which was irradiated for the short term test of the Am-1 experiment. Since a long-term irradiation test of the Am-1 experiment is now being planned, other long-term irradiated fuels from steady-state irradiation tests were examined by PIE in order to evaluate influence of Si impurity on cladding corrosion. These fuels were low density uranium–plutonium MOX fuels containing the same amount of Si impurity as the Np–Am–MOX fuel, in addition to less than 1% Am content.

The present results will be useful in the thermal design of fuel pins and in optimizing the fuel specifications of MOX fuels containing minor actinides.

## 2. Experimental

The fuel pellets were manufactured at an alpha particle tight glove box facility in the Nuclear Fuel Cycle Engineering Research Institute. Fuel specifications are shown in Table 1. Although a large amount of Si impurity, 1100 ppm Si, was contained in the fuels (Np–Am–MOX, MOX-1 and MOX-2), the fuel design specification (Si < 1400 ppm) was satisfied. The large amount of Si impurity was introduced by the use of a silicon-lined ball mill to crush the raw powder in the pellet fabrication process. The chemical form of Si impurity in the MOX fuel was assumed to be $SiO_2$.

The fuel pellets were inserted along with insulator pellets, a spring and other parts into a cladding tube of PNC-316 which

* Corresponding author. Tel.: +81 29 267 4141; fax: +81 29 267 7130.
*E-mail address:* maeda.koji@jaea.go.jp (K. Maeda).

0022-3115/$ - see front matter © 2008 Elsevier B.V. All rights reserved.
doi:10.1016/j.jnucmat.2008.10.020

**Table 1**
Typical fuel specifications and irradiation conditions.

| Irradiation test | Fuel type | $x/L$[a] (–) | Np (wt%) | Am (wt%) | Pu (wt%) | $^{235}U$ (wt%) | O/M ratio (–) | Fuel density (%TD) | Si content (ppm) | Burnup (at.%) | LHR[b] ($Wcm^{-1}$) | Clad temp.[c] (°C) |
|---|---|---|---|---|---|---|---|---|---|---|---|---|
| *Am-1experiment* | | | | | | | | | | | | |
| First test | Np–Am–MOX | 0.50 | 2 | 2 | 30 | 8.3 | 1.98 | 93 | 1100 | 0.008 | 427 | 595 |
| | MOX | 0.68 | – | 0.6 | 30 | 9.73 | 1.98 | 93 | 240 | 0.007 | 415 | 622 |
| *Am-1experiment* | | | | | | | | | | | | |
| First and second test | Np–Am–MOX | 0.50 | 2 | | 30 | 8.3 | 1.98 | 93 | 1100 | 0.037 | 429 | 571 |
| | Np–Am–MOX | 0.50 | 2 | | 30 | 8.3 | 1.95 | 93 | 1100 | 0.026 | 426 | 570 |
| *SS[d] irradiation tests* | | | | | | | | | | | | |
| MOX-1 | MOX | 0.50 | – | 0.3 | 30 | 21.5 | 1.98 | 85 | 1100 | 4.52 | 480 | 586 |
| MOX-2 | MOX | 0.50 | – | 0.9 | 30 | 21.5 | 1.99 | 85 | 1100 | 3.05 | 410 | 522 |

[a] Distance $x$ from fissile column bottom, fissile column length L.
[b] Linear heating rate.
[c] Inner wall.
[d] Steady-state.

was 20% cold-worked. The diameter and wall thickness of the cladding tube were 6.5 mm and 0.47 mm, respectively. The fissile column length of the Np–Am–MOX fuel pin was 200 mm; the other pins had a 550 mm fissile column length. The Np–Am–MOX fuel pellets were placed in the mid-section of the fissile column, and MOX fuel pellets (ref-MOX) used as a reference were placed in the rest of the column. In addition, the Np–Am–MOX fuel pellets stack length irradiated only in the first test was 40 mm ($x/L$ from 0.4 to 0.6), and the length irradiated in both the first and second tests was 72 mm ($x/L$ from 0.32 to 0.68). Here, $x$ and $L$ signify the distance from the fissile column bottom to the axial position and the length of the fissile column.

The local burnup and linear heat rating of the fuels are shown in Table 1, too. All the linear heat ratings were more than 410 $Wcm^{-1}$ at the beginning of fuel life, which was high enough for occurrence of fuel restructuring. The Np–Am–MOX fuels of the Am-1 experiment were irradiated twice for a very short time, and MOX fuels (MOX-1 and MOX-2) were long-term irradiated under steady-state conditions in which local burnup reached 4.52 at.%.

Two short-term irradiation tests for the Np–Am–MOX fuels were conducted as follows in the experimental fast reactor Joyo. In the first test, the reactor power was held for 10 min at the maximum level, then the reactor underwent rapid manual shutdown to preserve the fuel microstructure and to prevent additional fuel restructuring. In the second test, the reactor power was carefully raised in the same manner as had been done in the first test, and then the reactor power was held for 24 h at the maximum level, after which it was shut down via the normal procedure.

After the non-destructive PIE, the fuel pins were transversely and longitudinally sectioned for metallographic examinations and observations with an optical microscope and a scanning electron microscope (SEM). Specimens were mainly taken from the central part of the fissile columns and were done mainly on the central region which had been exposed to high temperatures, the fuel-cladding gap region and the fuel cracks. In addition, surface analysis on the fuels was carried out by electron probe micro analyser (EPMA) to obtain the distributions of Si, fission products (FPs) and constituents of fuel and cladding.

## 3. Results and discussion

Figs. 1(a) and (b) show optical micrographs of the fuel pin which was irradiated in the first test. Fuel restructuring of both Np–Am–MOX and reference MOX fuels had already started within this brief 10 min irradiation at the high linear heat rating.

At $x/L$ = 0.50 of the Np–Am–MOX fuel, relocation of some radially cracked pellets that resulted in gap closure was seen. The degree of the relocation was insignificant, because the gap closure easily occurred due to the narrow as-fabricated fuel-cladding gap which was 140 μm in diameter. However, a certain volume of the gap from the fuel relocation was involved in the volume of the central void. Movements of lenticular voids were not seen in the region of high temperatures and lenticular voids were only nucleated from the outer end of the columnar grains. Instead of lenticular voids, a number of spherical and cylindrical pores were found to be generated in the region of high temperatures. Thus, the columnar grain structure was found to be generated in spite of the absence of lenticular voids.

At $x/L$ = 0.68 of the reference MOX fuel, fuel relocation and the formation of a small central void were also observed. And some trails from migration of lenticular voids along fuel cracks were observed. However, in comparison with the Np–Am–MOX fuel, marked fuel restructuring did not occur. The radial position of the outer end of the columnar grains in the reference MOX fuel was approximately equal to that of the Np–Am–MOX fuel. In the case of the Np–Am–MOX fuel, spherical pores were extensively dispersed in the region of high temperatures, and not so many pores reached the fuel center. This suggested that the formation of columnar grains in the Np–Am–MOX fuel began earlier than that of the reference MOX fuel.

Fig. 1(c) shows an optical micrograph of the Np–Am–MOX fuel pin which was irradiated in both the first and second tests. At $x/L$ = 0.50 of the Np–Am–MOX fuel, neither the spherical pores nor cylindrical tubular pores were seen around the central void or at the region of high temperatures. The evidence of migration of lenticular voids from the outer end of the columnar grains to the fuel center was seen in specimens of the Np–Am–MOX fuel of O/M ratio 1.95. This suggested that the movement of lenticular voids to the fuel center occurred during the second test.

Many greyish inclusions were seen in the interiors of the spherical and cylindrical tubular pores of the Np–Am–MOX fuel. The distribution of elements across the spherical pores of the Np–Am–MOX fuel as analysed by EPMA is shown in Fig. 2. Concentrations of Pu, Am and Si, in addition to O, were locally high in the spherical pores. Generally the migrations of Pu and U occur through the gas phase in migrating pores by the mechanism of vaporization and condensation. In addition to fuel constituents, migration of Si impurity in the pores along the thermal gradient occurred. Thus Si-rich inclusions were concentrated in the migrating spherical and cylindrical tubular pores as well as in the grain boundary of

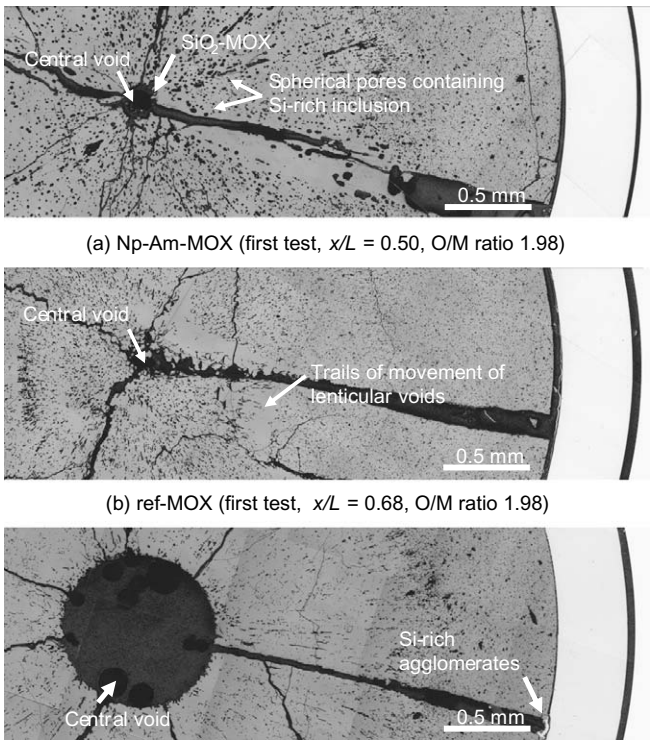


**Fig. 1.** Comparison of fuel microstructures in the Np–Am–MOX and ref-MOX fuels.

the columnar grains. The increase in concentration of Si-rich inclusions in the pores during the migration to the center resulted in coalescing and enlargement of the pores. Thus the pores acted as the main carriers of the Si-rich greyish inclusions to the center.

Additionally, coarse large grains in the region of high temperatures were surrounded by Si-rich greyish inclusions. Thus, existence of an appreciable amount of liquid phase of Si-rich inclusions between fuel grains was indicated. It was reasonable to think that during grain growth in the region of high temperatures, Si-rich inclusions were excluded to the grain boundary and

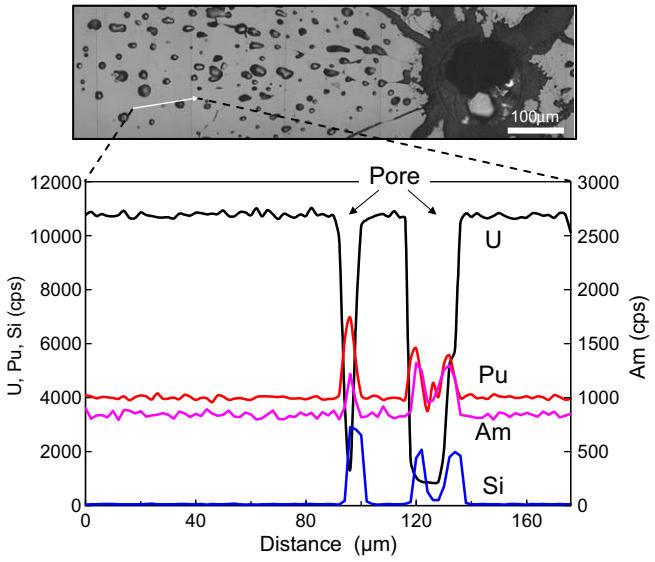


**Fig. 2.** Radial distributions of U, Pu, Am and Si across a spherical pore in the Np–Am–MOX fuel (first test, $x/L = 0.5$, O/M = 1.98).

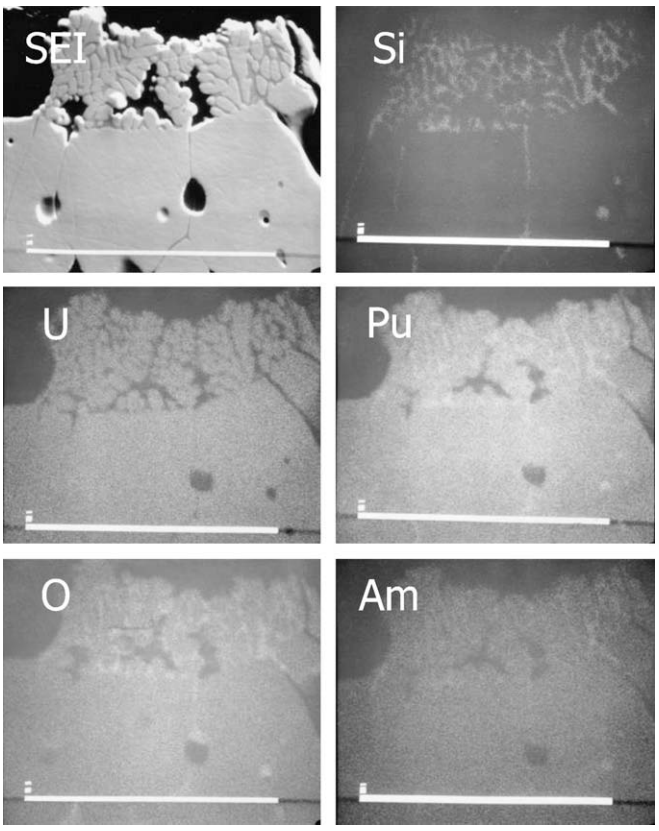


**Fig. 3.** EPMA X-ray maps of elements around the central void of the Np–Am–MOX fuel (first test, $x/L = 0.5$, O/M = 1.98).

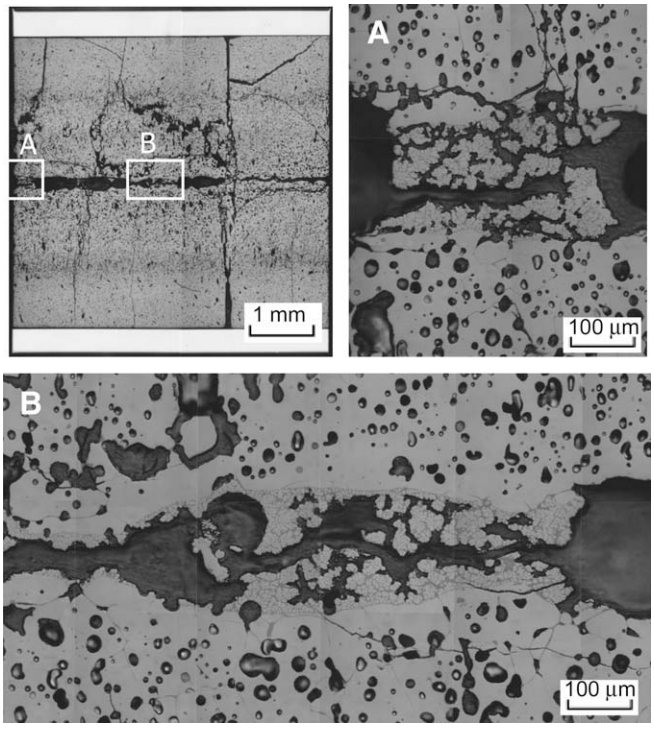


**Fig. 4.** Optical micrographs of the Np–Am–MOX fuel (first test, longitudinal specimen, $x/L = 0.51–0.64$, O/M = 1.98).

grains were elongated along the thermal gradient. The elongation of the grains in the direction of the temperature gradient resulted

in the columnar grain shape. Migration on grain boundaries of spherical and cylindrical pores was faster in comparison with migration within intragranular pores.

In spite of the occurrence of fuel cracking and relocation, movements of lenticular voids at the region of high temperatures were not detected in the Np–Am–MOX fuel pin of the first test. The following two reasons were considered responsible for this. (1) The radial and circumferential fuel cracks are generally the source of the disk-shaped voids [3]. However, the disk-shaped pores which develop into lenticular voids [4] were not generated because the degree of relocation by fuel cracking was restrained by the narrow as-fabricated fuel-cladding gap. (2) Si-rich inclusions were retained in the spherical and cylindrical tubular pores during fuel restructuring. Thus, the pre-existing sintered pores were sites for retaining Si-rich inclusions during the radial migration. This behavior of Si-rich inclusions prevented the pores from developing lenticular voids which migrate up the thermal gradient as a result of the vaporization and condensation mechanism.

Rapid reactor shutdown in the first test preserved the existing microstructure of the region of high temperatures by freezing. The dendritic structure of the eutectic phase was present in the interior of the central void of the Np–Am–MOX fuel. By contrast no sign of such a eutectic reaction was detected in the reference MOX fuel. The existence of the eutectic phase in the Np–Am–MOX fuel was assumed to be due to the presence of minor actinides, but mainly a large amount of Si impurity in the fuel. The eutectic phase existing around the central void of the Np–Am–MOX fuel at $x/L = 0.5$ was analysed by EPMA. Characteristic X-ray maps of the detected elements around the central void are shown in Fig. 3. The dendritic fuel constituents (MOX) as primary crystals and the Si-rich phase surrounding the primary crystals were detected. It was found that the eutectic phase was locally formed by the eutectic reaction of MOX–$SiO_2$. The morphology of the eutectic phase was similar to that of the $UO_2$–$SiO_2$ which was reported by Lungu et al. [5].

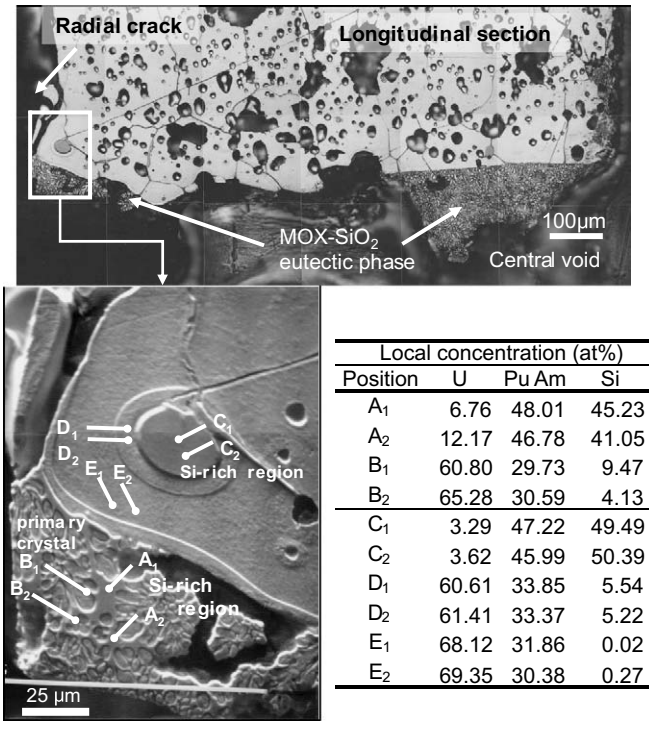


| Local concentration (at%) | | | |
|---|---|---|---|
| Position | U | Pu Am | Si |
| $A_1$ | 6.76 | 48.01 | 45.23 |
| $A_2$ | 12.17 | 46.78 | 41.05 |
| $B_1$ | 60.80 | 29.73 | 9.47 |
| $B_2$ | 65.28 | 30.59 | 4.13 |
| $C_1$ | 3.29 | 47.22 | 49.49 |
| $C_2$ | 3.62 | 45.99 | 50.39 |
| $D_1$ | 60.61 | 33.85 | 5.54 |
| $D_2$ | 61.41 | 33.37 | 5.22 |
| $E_1$ | 68.12 | 31.86 | 0.02 |
| $E_2$ | 69.35 | 30.38 | 0.27 |

**Fig. 5.** Optical micrograph and EPMA results for a chemically etched longitudinal specimen of the Np–Am–MOX fuel (first test, O/M = 1.98).

Observations of longitudinal sections were carried out in all the remnants of the Np–Am–MOX fuel column which had been irradiated in the first test. The locally formed eutectic phase in the interior of the central void is shown in Fig. 4. The large spherical pores were involved in delivering the Si-rich inclusions to the central void, and the MOX–$SiO_2$ eutectic reaction occurred at the interior of the central void. No significant axial movement of the MOX–$SiO_2$ eutectic phase was detected. Moreover no unexpected findings such as the axial movement of fuel constituents which might influence the fuel integrity were detected by the gamma scan test.

Photographs of OM and SEM for a chemically etched longitudinal specimen are shown in Fig. 5. A thin layer of fuel microstructure was axially formed along the inner wall of the central void. This characteristic microstructure indicated the boundary of molten Si-rich inclusions and the fuel matrix; the microstructure was also observed at the spherical void near the central void. The results of quantitative analysis by the EPMA at the fuel center are also shown in the Table of Fig. 5. Locally concentrated Si-rich inclusions which accompanied Pu and Am, in addition to O, were detected in or near the central void. The sum of the concentrations of the elements existing in the Si-rich region such as Am, Pu and Si was more than 90 at.%. A preliminary calculation showed the fuel centerline temperature was more than 2400 °C. The phase diagram of $UO_2$–$SiO_2$ has been reported [5,6]. The MOX and $UO_2$ have a similar melting point. Thus the phase diagram reported in refs. [5,6] suggested that the high concentration of Si-rich inclusions and a high temperature made it possible to form the eutectic phase. Am and Pu were locally concentrated in the Si-rich phase. However the chemical form of Am, Pu, Si and O were not determined; these elements are known to form silicates, such as $AmSiO_4$ and $PuSiO_4$ [7]. This suggests that silicates could have formed during the solidification of the molten mixture of the Si-rich inclusions.

As shown in Fig. 1(c), greyish agglomerates and a shallow attack on the inner wall of the cladding were observed at a crack opening in the Np–Am–MOX fuel pin which experienced the second test. The fuel cracks were developed during heating to the operating temperature or during cooling from it. The EPMA X-ray maps which were obtained from around the crack opening and the fuel-cladding gap of the Np–Am–MOX fuel indicated that the greyish agglomerates were composed of Si-rich compounds. The grain boundaries of the cladding at the attacked position were essentially free from reaction products. The Si-rich agglomerates were probably formed due to the vaporization of SiO to a colder region of the fuel during the second test. Otherwise the movement of the Si-rich inclusions towards the cladding occurred through the fuel cracks.

Fig. 6 shows an optical micrograph and EPMA X-ray maps obtained from the normal MOX fuel (MOX-1) which was irradiated under steady-state conditions; it contained a large amount of Si impurity. The greyish Si-rich agglomerates at the crack opening and attacks on the inner wall of the cladding which accompanied the exfoliation of the cladding were also observed in both the MOX-1 and MOX-2 fuels. Formation of the greyish Si-rich agglomerates as shown in Fig. 6 were probably attributed to the vaporization of SiO in the high temperature region of the MOX-1 fuel. In addition, cladding constituents (Fe, Ni and Cr) and FPs (Cs, Te, Ba) were also present in the fuel-cladding gap. Some Si was present together with Cs and O. Residual Si was present together with metallic Fe, Cr and Ni. However, the shallow attack on the inner wall of the cladding in the MOX-1 fuel was similar to that of the Np–Am–MOX fuel which experienced the second test, and seemed to have remained after the fuel restructuring. The Fe, Si and O in the agglomerates could form $Fe_2SiO_4$, which suggested it prevented the cladding from significant corrosion which could occur by accumulation of FPs.

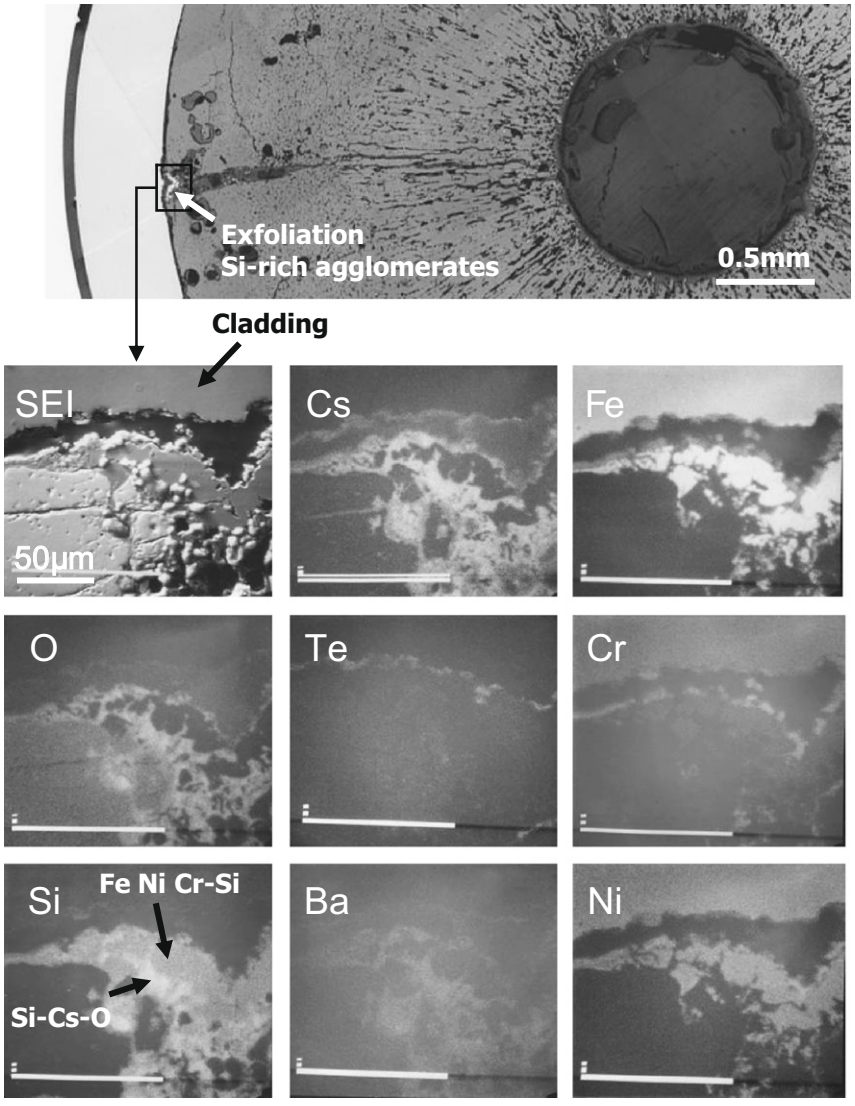


**Fig. 6.** Optical micrograph and EPMA X-ray maps of elements in the crack opening and cladding inner wall (MOX-1 fuel, 0.3 wt%-Am, O/M = 1.98).

By contrast, the grain boundary corrosion of the cladding which is known as cladding component chemical transport (CCCT) [8] was detected in MOX-2 fuel. It was attributed to the higher oxygen potential than in the MOX-1 fuel, which was derived from both of the Am content (0.9 wt%) and fuel compositions nearly stoichiometric in the MOX-2 fuel [9]. However, grain boundary corrosion of the cladding inner wall at the crack opening occurred selectively and was marked by the release of reactive FPs such as Cs and Te in comparison with other cladding wall regions. Also, the amount of Si-rich agglomerates at the crack opening of the MOX-2 fuel was smaller than that in MOX-1 fuel, because the central void in the former was smaller than that of the latter. It was reasonably understood that the amount of Si-rich agglomerates was increased depending on the degree of fuel restructuring. In addition exfoliation of a thin layer, composed mainly of Fe, Si and O, was seen. Under the exfoliated $Fe_2SiO_4$ thin layer of some fuel particles, Cs and Te were present on the inner wall of the cladding. It was possible that corrosion proceeded selectively at the crack opening by accumulation of FPs. Moreover it was thought that the grain boundary corrosion of the cladding was selectively developed by the volatile corrosive elements Cs and Te after the thin protective $Fe_2SiO_4$ layer exfoliated or that the amount of Si was insufficient to protect the surface which was attacked by Si-rich agglomerates. The exfoliation of the layer seemed to have occurred by partitioning the fuel bonding to the cladding during cyclic reactor operations.

## 4. Summary and conclusions

Irradiation behavior of Si impurity was examined by PIE mainly for Np–Am–MOX and normal MOX fuels.

Short-term irradiation behavior of Si impurity was examined for the Np–Am–MOX fuel. Si impurity, accompanied by Am, Pu and O, was transported by the spherical pores and the cylindrical tubular pores to the fuel center during fuel restructuring, where a eutectic reaction of fuel and enriched Si occurred. Migration of lenticular voids along the thermal gradient was seen and the columnar grains were more developed after the transportation of Si impurity from the region of high temperatures. After fuel restructuring, Si-rich agglomerates without fuel constituents were deposited at the fuel crack openings. Shallow attacks on the inner wall of the cladding by the agglomerates were observed.

Long-term irradiation behavior of Si impurity as related to cladding attack was examined for the normal MOX fuels. Steady-state long-term irradiated fuels showed shallow attacks on the inner wall of the cladding that were likewise observed near the location of fuel cracks. A shallow attack of the inner wall of the cladding in

the MOX-1 fuel was considered to have remained after fuel restructuring. And a protective layer of $Fe_2SiO_4$ was locally present on the inner wall of the cladding near the fuel cracks after a large amount of Si-rich inclusions was agglomerated at the crack opening. However, grain boundary corrosion of the cladding wall at the crack opening by cladding component chemical transport (CCCT) selectively and markedly occurred in comparison with other cladding wall regions of the MOX-2 fuel.

## Acknowledgements

The authors wish to gratefully acknowledge the contributions of Y. Ohsato, Y. Onuma, S. Nukaga (Nuclear Technology and Engineering Corporation) for conducting the destructive PIE.

## References

[1] T. Sekine, T. Soga, D.W. Wootan, S. Koyama, T. Aoyama, Short Term Irradiation Test of Fuel Containing Minor Actinides Using the Experimental Fast Reactor Joyo, in: GLOBAL 2007, Boise, Idaho, USA, 9–13 September 2007.
[2] K. Maeda, S. Sasaki, M. Kato, Y. Kihara, Short-term irradiation behavior of Np/Am–MOX fuel irradiated in the experimental fast reactor Joyo, in: E-MRS 2008 Spring Meeting, Strasburg, France, 26–31 May 2008.
[3] P.F. Sens, J. Nucl. Mater. 43 (1972) 293.
[4] C. Ronchi, C. Sari, J. Nucl. Mater. 50 (1974) 91.
[5] S. Lungu, I.L. Beleută, D. Apostol, O. Rădulescu, J. Nucl. Mater. 48 (1973) 165.
[6] S. Lungu, I.L. Beleută, J. Nucl. Mater. 35 (1970) 35.
[7] J.J. Kats, G.T. Seaborg, L.R. Morss, The Chemistry of the Actinide Elements, 2nd ed., Chapman and Hall Ltd, New York, 1986. p. 721 and 907.
[8] M.G. Adamson, E.A. Eitken, R.W. Caputi, P.E. Potter, M.A. Mignanelli, Thermodyn. Nucl. Mater. 1 (1979) 503.
[9] M. Osaka, K. Kurosaki, S. Yamanaka, J. Nucl. Mater. 357 (2006) 69.